Received: 7 February 2022 | Revised: 15 March 2022 | Accepted: 12 April 2022

DOI: 10.1002/jmr.2960

RESEARCH ARTICLE

Journal of Molecular Recognition WILEY

Sensitive recognition of prostate-specific antigen using biotinylated antibody encapsulated on *D*-penicillamine decorated wrinkled silicate nanoparticles (WSN): An innovative sandwich-type biosensor toward diagnosis of prostate cancer

Milad Baghal Behyar[1,2] | Fatemeh Farshchi[3] | Mohammad Hasanzadeh[1,4]

[1]Pharmaceutical Analysis Research Center, Tabriz University of Medical Sciences, Tabriz, Iran

[2]Food and Drug Safety Research Center, Tabriz University of Medical Sciences, Tabriz, Iran

[3]Drug Applied Research Center, Tabriz University of Medical Sciences, Tabriz, Iran

[4]Nutrition Research Center, Tabriz University of Medical Sciences, Tabriz, Iran

Correspondence
Mohammad Hasanzadeh, Pharmaceutical Analysis Research Center, Tabriz University of Medical Sciences, Tabriz, Iran.
Email: hasanzadehm@tbzmed.ac.ir

Funding information
Tabriz University of Medical Sciences

Abstract

In this study, a new sandwich-type biosensor was developed to specific recognition of prostate-specific antigen (PSA) and early-stage diagnosis of prostate cancer using encapsulation of biotinylated antibody (Ab1) of prostate-specific antigen on *D*-penicillamine decorated wrinkled silicate nanoparticles (WSN). For the first time, KCC-1-NH-DPA was synthesized and used to immobilization of biomacromolecules. So, fabricated immunosensor was performed by on sandwich-type strategy. After fabrication of immunosensor, cyclic voltammetry, differential pulse voltammetry, and square wave voltammetry techniques were used to electrochemical evaluation of immune-platform for PSA detection. The proposed biocompatibility immune-platform provided a novel interface toward sensitive bioanalysis of PSA biomarker in human plasma samples. Due to the use of gold nanoparticles functionalized Cysteamine (Cys A) in the structure of the secondary antibody (Ab2 [HRP-Ab2]), the intensity of the electrochemical signal has increased, resulting in a more accurate detection of the target molecules. Under the right conditions, the engineering immunosensor provides good bioanalytical performance for determining the PSA biomarker in the linear range of 0.002 to 60 μg L^{-1} which low limit of quantification was 0.002 μg L^{-1}. As a result, it is suggested to use these immune-devices in the clinical pre-diagnosis of prostate cancer.

KEYWORDS
advanced nanomaterials, bioanalysis, biomacromolecules, biomarker, biosensor, prostate cancer

1 | INTRODUCTION

The second most communal cancer in the world among men is prostate cancer.[1] Prostate cancer is the one of the furthermost communal malignancy in humans and it is one of the leading causes of cancer deaths in the world.[2] Based on the obtained results, there is currently there is no definitive cure for cancer and early diagnosis is especially important[3] Different methods are now used to diagnose prostate cancer.[4] These include prostate imaging (rectal testing), biopsy, and prostate-specific antigen (PSA) screening.[5] Among the mentioned methods, rectal test and biopsy are unpleasant for the patient and the doctor, and they are also considered as invasive methods.[5] Biomarker molecules are very important in the treatment and early diagnosis of cancer.[6] PSA is an important biomarker in the early detection and diagnosis of prostate cancer.[7] In particular, there are several techniques for the detection of PSA such as enzyme-linked immunosorbent assays (ELISA), piezoelectric and optical.[8] However, these methods have some limitation such as low efficacy, high cost, and

imprecise results.[9] In the meantime, an electrochemical immunosensor with high potential is used for primary diagnosis of prostate cancer.[10] Electrochemical immunosensors have great compensations including low cost, fast detection, high sensitivity, and high selectivity.[11]

Advanced nanomaterials have a significant role in the development of electrochemical immunosensors.[12] In this regard, wrinkled fibrous nano-silica (WFNS) have attracted the attention of electrochemical immunoassay devices.[13] WFNS nanomaterials have been noted for their easy synthesis, adjustable particle size, large pore volume, excellent mechanical stability, low toxicity, complete biocompatibility, adjustable pore size, and unique large surfaces.[14] In the WFNS structure, the fibers resemble porous spheres that have a very accessible surface.[14] The WFNS was prepared in a recently published study by Polshettiwar and coworkers.[15,16]

In this study, an innovative sandwich-type immunosensor was developed to specific recognition of prostate-specific antigen (PSA) and early-stage diagnosis of prostate cancer using encapsulation of biotinylated antibody (Ab1) of prostate-specific antigen on *D*-penicillamine decorated wrinkled silicate nanoparticles (WSN). For the first time, KCC-1-NH-DPA was synthesized and used to the immobilization of biomacromolecules. So, fabricated immunosensor was performed by on sandwich-type strategy. After fabrication of immunosensor, cyclic voltammetry, differential pulse voltammetry, and square wave voltammetry techniques were used to electrochemical evaluation of immune-platform for PSA detection. The proposed biocompatibility immune-platform provided a novel interface toward sensitive bioanalysis of PSA biomarker in human plasma samples. Due to the use of gold nanoparticles functionalized Cysteamine (Cys A) in the structure of the secondary antibody (Ab2 [HRP-Ab2]), the intensity of the electrochemical signal has increased, resulting in a more accurate detection of the target molecules. As a result, it is suggested to use this immune-devices in the clinical pre-diagnosis of prostate cancer.

2 | EXPERIMENTAL

2.1 | Chemicals and elements

N-hydroxysuccinimide, 1-ethyl-3-(3-dimethylaminopropyl) carbodiimide, 3-aminopropyl triethoxysilane (APTES), dipenicillamine (DPA), EDC/NHS, Toluidine Blue (TB), Chitosan, $AgNO_3$, Acetic acid, Sulfuric acid, Cysteamine hydrochloride, Bovine Serum Albumin (BSA), and Glutaraldehyde purchased from Sigma-Aldrich, Urea, Sodium dihydrogen phosphate, Acetone, Potassium ferrocyanide, Potassium chloride, Hexanol, Potassium hexacyanoferrate (III), Tetraethyl orthosilicate (TEOS), Cetyl trimethylammonium bromide (CTAB), Dried toluene, Ethanol, Cyclohexane, N,N-dimethyl sulfoxide (DMSO) were produced by the German company Merck, Disodium hydrogen phosphate were produced by the scharlau spain company. CA 15-3, CEA antigen, Human PSA ELISA kit including different concentration of PSA antigen, HRP Labeled anti-PSA, biotinylated antibody, standard buffer, wash solutions, were obtained from CanAg Diagonestic AB Technology Co., HA and SNCA antigen were purchased from ZellBio GmbH. Also, for real sample analysis, human plasma samples were found from plasma blood transfusion research center (Tabriz, Iran). All of synthesize procedure of nanomaterials have been explained in supporting information.

2.2 | Instruments

Electrochemical analyses and electro polymerization have been done by using conventional three-electrode organization. In this way, a glassy carbon electrode (GCE) was used as a working electrode ($d = 2$ mm), a platinum wire employed as an auxiliary electrode, and Ag/AgCl used as a reference electrode in the Electrochemical cell. The electrodes were prepared from the Azar electrode and then connected to Auto lab PGSTAT302N and evaluated by Nova 1.11 software. The morphology and topographical images of the prepared electrodes were obtained by FE-SEM (Field emission scanning electron microscopy) and also, EDS (energy dispersive spectroscopy) was employed to identify the elements on the surface of the electrodes.

2.3 | Encapsulation of the biotinylated antibody (Ab1) into KCC-1-NH_2-DPA

In this part of biosensor preparation, 0.001 g of KCC-1-NH_2-DPA was dispersed in 100 μL of PBS and placed on an ultrasonic bed for 10 minutes to completely dissolve the nanoparticles. The resulting solution was then mixed with 300 μL of Ab1 and mixed at room temperature for 24 hours. Then, the resulting solution was centrifuged at 6000 rpm for 5 minutes and the supernatant was gathered for use and kept at 4°C. Figure 1A-H, displays the diffusion of biotin-containing antibodies (Ab1) into KCC-1-NH_2-DPA cavities can be confirmed by FE-SEM at different magnifications. Also, the presence of C, O, Si, P, and S was confirmed by energy scattering spectroscopy (EDS) (Figure 1I) and elemental scattering map (MAP) analysis (Figure 1J).

2.4 | Preparation of the secondary antibody (HRP-Ab2/Cys A-AuNPs/TB/Glutaraldehyde)

Initially, Cys A-AuNPs were synthesized. For further explanation, in 20 μL of deionized water, 40 μL of (0.5 M) Hydrogen tetrachloroaurate(III) hydrate ($HAuCl_4{\cdot}3H_2O$) were completely dissolved and heated until they reached boiling point. On the other hand, TSC (0.5 M) was dissolved in 20 mL of DW. The resulting solutions were then combined and incubated for 20 minutes. Then 1 mL of aqueous Cys A solution was added to the prepared combination to obtain Cys A-AuNPs. The bond between AuNPs and Cys A is covalent. After obtaining Cys A-AuNPs, 500 μL of Cys A-AuNPs, 5 μL of HRP-Ab2, and 10 μL of GLU were combined and incubated at 4°C for 12 hours. Then, 100 μL of TB (2 mM) was combined with 1 mL of the

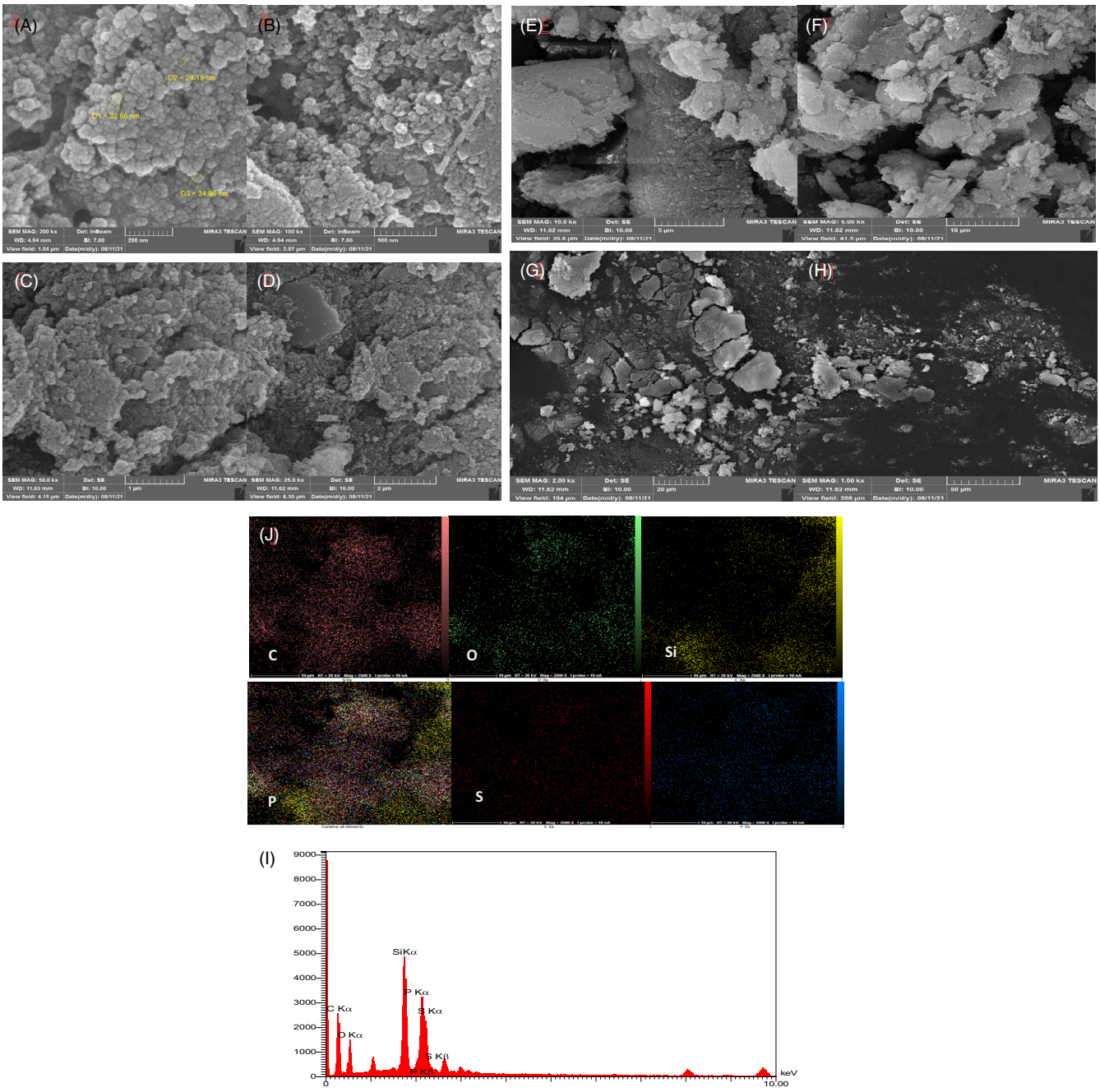

FIGURE 1 (A-H) FE-SEM images of KCC-1-NH_2-DPA-Ab1 deposition at different scales. (I) EDS of bare KCC-1-NH_2-DPA-Ab1 and (J) MAP of bare KCC-1-NH_2-DPA-Ab1

prepared solution. Then, 20 μL of BSA was combined with the prepared solution to block unoccupied active sites to increase sensitivity. Finally, 20 μL of phosphate buffer solution (PBS) was poured into the solution and incubated for at least 0.5 hour at 4°C.

2.5 | Preparation of real samples

Human plasma samples were used to determination PSA in real samples. Therefore, 10 μL of different concentrations of PSA antigen was mixed with the 10 μL of human plasma sample. To obtain a clear supernatant, the solution was centrifuged at 10 000 rpm for 5 minutes and kept in a clean microtube.

2.6 | Pre-treatment of the GCE

The surface of the GCE was cleaned and gently polished with alumina for 10 minutes. The surface of electrodes was put in dilute H_2SO_4 solution for 10 minutes. After 10 minutes, electrodes were immersed

in the distilled water and then placed in a solution of water and acetone for 10 minutes. Lastly, the surface of the electrodes was washed with DW and let them to dry at room temperature.

2.7 | Fabrication of the sandwich-type immunosensor

After preparing and cleaning the surface of the GCE, a poly chitosan (P[CS]) coating was applied on the surface of the electrode. For more information, 0.005 g of chitosan was dissolved in solvent (10 mL of deionized water+5 μL of acetic acid), then 10 mL of chitosan solution was dumped into the electrochemical cell and the coating layer was performed for up to 20 cycles (Scan rate = 50 mV/s, the potential range from −1 to 1 V) (Figure 2). The surface of the electrodes was then washed with distilled water. In the second step, for the coating of silver nanoparticles (AgNPs), 0.001 g of $AgNO_3$ was mixed in a solvent (10 mL of DW + 60 μL of nitric acid) and then the prepared solvent was placed in the electrochemical cell and the coating layer was used using the Cyclic voltammetry technique was performed for up to 30 cycles (scan rate = 100 mV/s, the potential range from −1 to 0.1 V) (Figure S7). KCC-1-NH_2-DPA-Ab1 was combined with NHS/EDC in a ratio of 1:2 and incubated on the surface area of AgNPs-P(CS)-GCE for 1 hour. The NHS/EDC solution acts as an activator of the electrode matrix functional groups to create a suitable surface for antibody binding to the electrode substrate matrix. After incubation, the surface of the electrode was washed with a special buffer and 5 μL of BSA was incubated for 0.5 hour. This was done to block unreacted electrode sites and to minimize nonspecific bonding. After incubation, the electrode surface was washed with a special buffer to stop the reaction and remove possible contaminants, and 5 μL of PSA antigen was incubated for 1 hour and washed again with a special buffer for the electrode surface. In the last step, 5 μL of Ab2 was incubated on the PSA- BSA- KCC-1-NH_2-DPA-Ab1- AgNPs- P (CS)- GCE surface for 1 hour (Scheme 1). The electrode was kept at 4°C during incubation. Finally, for electrochemical evaluation and PSA detection, we place the electrode inside the electrochemical cell.

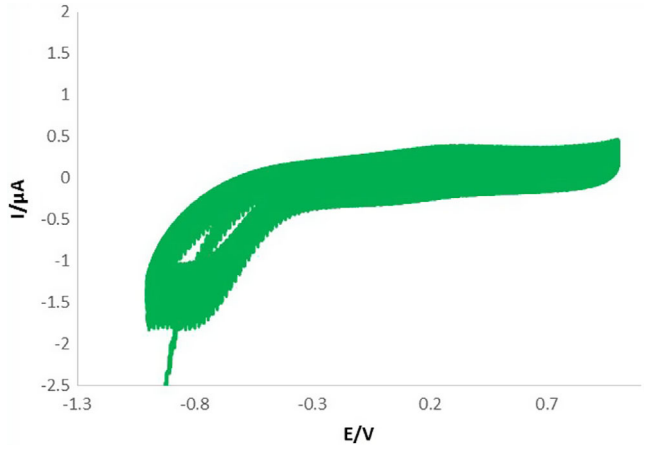

FIGURE 2 CVs for GCE in the presence of chitosan solution (10 mL DW + 5 μL acetic acid + 0.005 g chitosan) toward electropolymerization of P(CS) on the surface of GCE in the potential range of −1 to 1 V, scan rate of 50 mV s^{-1} using 20 cycles

3 | RESULTS AND DISCUSSION

3.1 | Morphology of modification surface

The surface morphology of the engineered immunosensor was examined by FE-SEM. Figure S8A-H (see supporting information) shows the FE-SEM images for P (CS)-GCE. From the images above, it is clear that a layer of P (CS) with a microsphere-like shape was dependent to the surface. The presence of chitosan polymer layer was also confirmed by EDS and the presence of O, C, and N elements in addition to EDS (Figure S8I) by MAP (Figure S8J). The advantages of P (CS), which is a natural polysaccharide, include increased surface adhesion, non-toxicity, and biocompatibility with other particles.[17] Figure S9 showed FE-SEM pictures with EDS and MAP of AgNPs on the surface of the P (CS) modified glass carbon electrode. By examining the results, the presence of a layer of silver nanoparticles on the external area of the P (CS)-GCE electrode at various magnifications can be detected. Silver spherical nanoparticles are clearly visible. Figure S10 shows images of FE-SEM, along with EDS and MAP, related to the KCC-1-NH_2-DPA-Ab1 nanoparticle activated with NHS/EDC on the surface of a GCE modified by AgNPs-P (CS). Carefully in the results, the occurrence of KCC-1-NH_2-DPA-Ab1 layer on the external area of AgNPs-P (CS)-GCE can be proved at different magnifications. Figure S11A-H shows FE-SEM images and Figure S11I shows EDS and Figure S11J shows MAP after PSA incubation on the surface of BSA-KCC-1-NH_2-DPA-Ab1-AgNPs-P (CS)-GCE. As can be seen from the figures, the chemical and morphological changes of the surface show the effective stabilization of the biological material on the surface of engineered electrode and the bioreceptor sample. Finally, Figure S12 shows the results of FE-SEM and analysis of EDS and MAP after incubation of Ab2 labeled with HRP enzyme. After the incubation of Ab2, a novel change in electrode surface morphology was observed, which confirmed the efficacious stabilization of the secondary antibody.

3.2 | Electrochemical behavior of immunosensor

To study the steps of development of the electrochemical immunosensor, the DPV and SWV techniques were used which supporting electrolyte is 0.01 M $[Fe(CN)_6]^{3-/4-}$/KCl. Evaluation of the results showed that after the polymerization of chitosan on the surface of the GCE, the peak current increases, that proves the efficacious coating layer of P (CS). After the deposition of silver nanoparticles (AgNPs) on the P (CS) layer, the peak current increased dramatically due to the high electrical conductivity of AgNPs.[18] After incubation of KCC-1-NH_2-DPA-Ab1 on the surface of the prepared electrode, the peak current decreases, which indicates the successful KCC-1-NH_2-DPA-

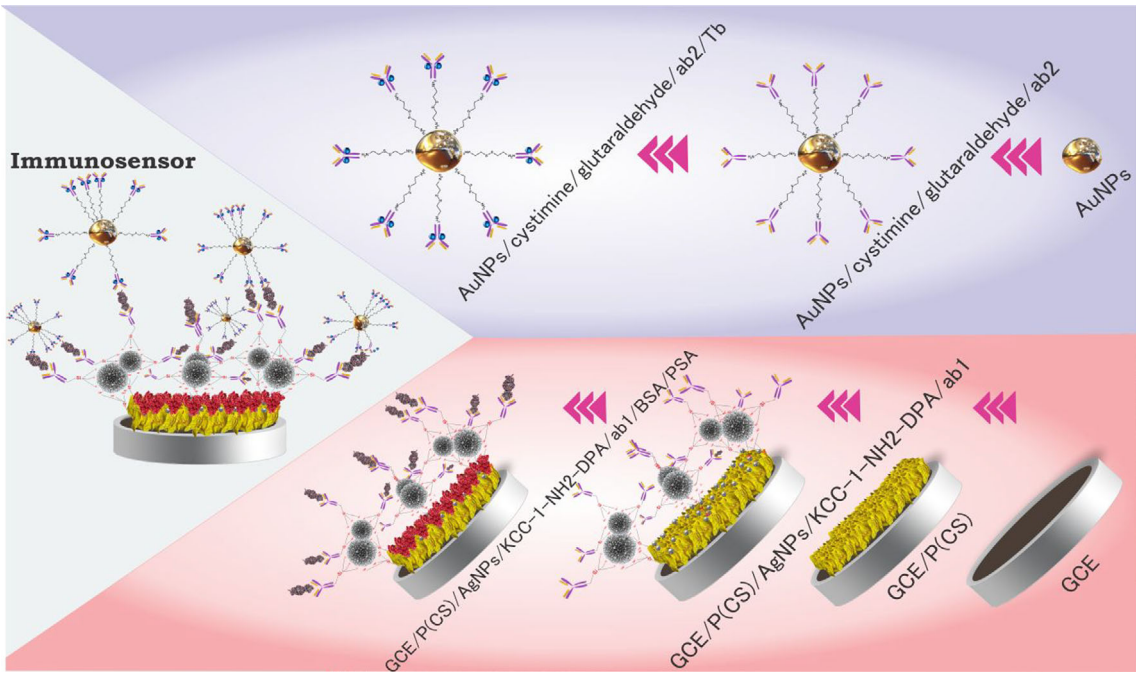

SCHEME 1 Illustration of the prepared sandwich immunosensor for the identification of PSA biomarker

Ab1 deposition layer. First, KCC-1-NH_2-DPA nanoparticles have poor conductivity and second, the electrode surface is blocked by anti-PSA antibody. Then, after incubation of biological materials (BSA and PSA), the peak current decreases, so that after the incubation of PSA antigen, the peak current reached a minimum, that shows the fruitful formation of antibody-antigen immunocomplex. The formation of this immunocomplex limits electron transfer. It should be said that, after incubation, the surface of PSA-BSA-Ab1-KCC-1-NH_2-DPA-AgNPs-P (CS)-GCE with CysA AuNPs-glutaraldehyde-toluidine blue-Antibody HRP (Ab2) peak current increased. This is related to the amplification of current by gold nanoparticles (AuNPs). The antibodies work as insulators so, they prevent the current from increasing too much (Figure 3).

3.3 | Analytical performance

To evaluate the analytical approach of the engineered electrochemical immunosensor, the differential pulse sensitive voltammetry technique at different concentrations of biomarkers was used and the ability of the technique to detect PSA biomarkers was evaluated. DPV method was used to detect different concentrations of PSA biomarkers (0.002 to 60 μg L^{-1}) in the presence of 0.01 M $[Fe(CN)_6]^{3-/4-}$/KCl as a support electrolyte. Figure 4 shows the DPVs of the prepared immunosensor along with the point diagram of the different concentrations of the PSA biomarker. According to the results, there is an inverse relationship between different concentrations of PSA marker and peak current intensity, so that with decreasing PSA concentration, the amount of electric current increases. The linear concentration range of the engineered immunosensor was 0.002 to 60 μg L^{-1}. Also, the obtained LLOQ was 0.002 μg L^{-1}. The linear regression calculation obtained from the point diagram for DPV was obtained:

The obtained linear regression from DPV calculation in standard samples:

$$I_p\,(\mu A) = 2.1683\,\mathrm{Log}\,C_{(PSA)} + 26.023,\ R^2 = 0.9933.$$

In Table 1,[19-25] the performance of previously reported immunosensors (biosensors) to determine the PSA biomarker was compared with the novel prepared electrochemical sandwich-type immunosensor.

Table 1[19-25] compares the analytical results with those of other electrochemical biosensors reported for the identification of PSA biomarkers. Comparison of the results with other PSA biosensors reported in Table 1 showed that the advantages of our developed electrochemical immunosensor are superior to PSA for five important reasons. The great results can be related to the above details: (a) The occurrence of a P (CS) polymer layer with properties such as increased surface adhesion, biocompatibility with other particles and non-toxicity. (b) The presence of a layer of AgNPs with the unique property of high electron transfer, which played an important role in better detection of PSA. (c) Homogeneous layer KCC-1NH_2-DPA-Ab1 structure with biotin antibody a suitable and efficient substrate for loading all kinds of biomarkers are excellent because they have a large pore volume for loading and will also act specifically due to the presence of antibodies. (d) Secondary antibodies containing AuNPs enhance the signal and better and more accurate biomarker detection. (e) Finally, shorter preparation time, simplicity of preparation steps and eco-friendly are other notable advantages.

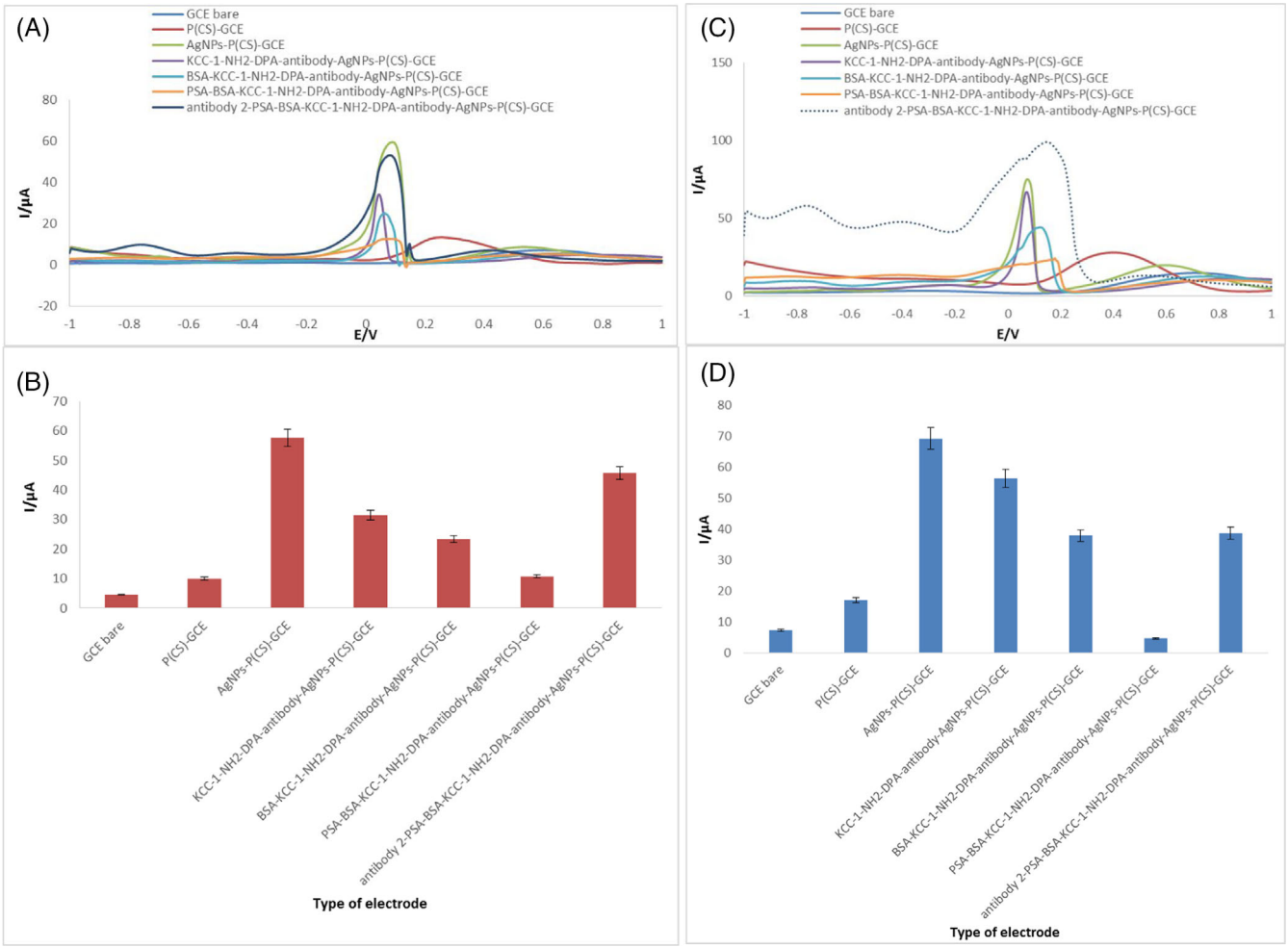

FIGURE 3 (A) DPVs and (C) SWVs of GCE bare, P (CS)- GCE, AgNPs-P (CS)-GCE, KCC-1-NH_2-DPA-Ab1-AgNPs-P(CS)-GCE, BSA-KCC-1-NH_2-DPA-Ab1-AgNPs-P(CS)-GCE, PSA-BSA-KCC-1-NH_2-DPA-Ab1-AgNPs-P(CS)-GCE, Ab2-PSA-BSA-KCC-1-NH_2-DPA-Ab1-AgNPs-P(CS)-GCE in the presence of supporting electrolyte 0.01 M $[Fe(CN)_6]^{3-/4-}$/KCl, potential range −1 to 1 V and the scan rate of 100 mV s^{-1} (B and D) Histogram of peak current vs type of electrode

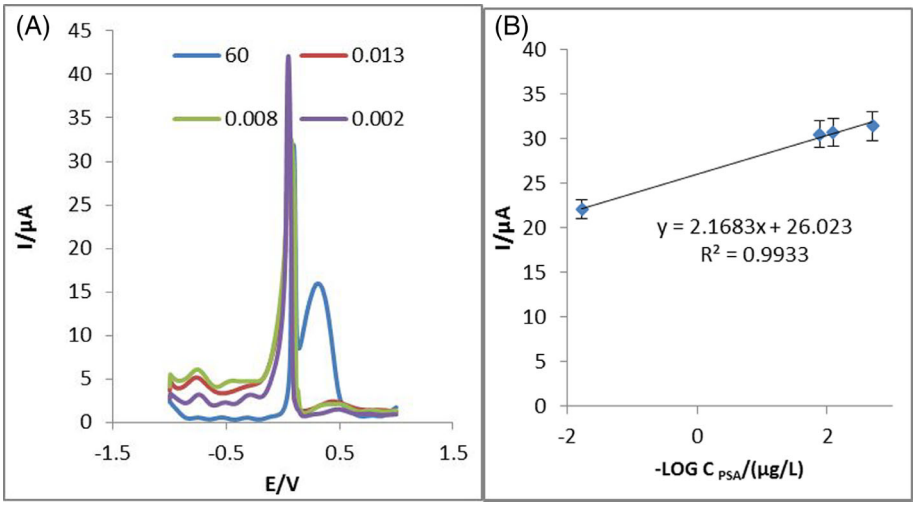

FIGURE 4 (A-B) DPVs of developed immunosensor on the present of different concentrations (60 − 30 − 10 − 2 − 0.1 − 0.07 − 0.03 − 0.013 − 0.008 − 0.005 − 0.002 µg L^{-1}) of PSA in the presence of supporting electrolyte 0.01 M $[Fe(CN)_6]^{3-/4-}$/KCl, potential range −1 to 1 V and the scan rate of 100 mV s^{-1}

TABLE 1 Comparison of the sensitivity and performance of the engineered immunosensor with other electrochemical immunosensors to determine PSA biomarker

Technique	Substrate	Linear range	LLOQ	Reference
Electrochemical	Coral-like poly-aniline (PANI)/gold nano-particles (AuNPs)	0.1 pg mL^{-1}-100 ng mL^{-1}	462.7 ng mL^{-1}	19
Electrochemical (DPV)	Peptide Biosensor Based on in SituSilver Deposition	0.001-30 ng mL^{-1}	0.001 ng ml^{-1}	20
Electrochemical (SWV)	Fe_3O_4-Ab1/Ag/CysA-AuNPsHRP-Ab2	0.01-1 μg L^{-1}	0. 01 μg L^{-1}	21
Electrochemical (EIS)	Glassy carbon electrode modified with TiO_2-rGO hybrid nanosheets	3-10^6 pg ml^{-1}	1 pg ml^{-1}	22
Electrochemical (DPV)	Paper based immunosensor based on Citrate AgNPs-GQDs nano-ink/Cys A)	10-0.05 μg L^{-1}	0.05 μg L^{-1}	23
	Paper based immunosensor based on conductive Ag-ink	60-0.09 μg L^{-1}	0.09 μg L^{-1}	24
	Label free based on SiO_2- AgNPs	0.03-0.001 μg L^{-1}	0.001 μg L^{-1}	25
	P(CS)-AgNPs-KCC-1-NH_2-DPA-Ab1-BSA-PSA-Ab2	0.002-60 μg L^{-1}	0.002 μg L^{-1}	This work

3.4 | Kinetic study

To obtain useful data including electrochemical mechanisms, the relationship between peak current intensity and scanning rate can be used. Scanning rate is important as one of the effective parameters in the redox evaluation of numerous compounds. To study the surface electrochemical behavior (AgNPs- P (CS) - GCE), CV technique to determine the effect of different scanning velocities without the analyte (PSA) and in the presence of 0.01 M $[Fe(CN)_6]^{3-/4-}$/KCl as a control solution in the range of 0.1 to 1 mV / s (Figure S13A (see supporting information)). As shown in the Figure S13, the peak current increases in proportion to the scan rate. The obtained linear regression equation is:

$$I_{pa}(\mu A) = 0.5777\, v^{1/2}(v.s^{-1}) + 18.422\left(R^2 = 0.3573\right).$$

Also, the linear regression equation between the $\ln I_{pa}$ and $\ln v$ was drawn, which is as follows:

$$\mathrm{Ln}I_{pa}\,(\mu A) = 0.2203\ln\nu\,(V.s^{-1}) + 2.0974\left(R^2 = 0.6444\right).$$

To evaluate the type of electrode process that is diffusion or adsorption, it should be noted that the slope is about 0.5 for the process controlled by diffusion and the is about 1 for the process controlled by absorption.[21] According to the description given, the slope of 0.2203 shows that the mass transfer of redox process on the surface of electrode is approximately controlled by diffusion (Figure S13E). It is noteworthy that the following equation was used to obtain the number of electrons moved from the anode potential peak against the Neperian logarithm of the scan rate.

$$Ep = \left(\frac{n^2f^2}{4RT}\right)\ln V + constant$$

Also, the values of the specific surface area covered by different electrodes are calculated by the cyclic voltammetry technique using the following formula.

$$Ip = \left(\frac{n^2f^2}{4RT}\right)vA\Gamma*$$

R is gas constant (8.314472 j K^{-1} mol^{-1}), * Γ is the covers the surface of redox species, F is Faraday constant (F = 96.487 C mol^{-1}), A is the electrode surface area (A = πr^2 = 0.0314 cm^2), v is (sweep rate) and T is the Kelvin temperature (298 K). By transferring the information in the above equation, Γ* was obtained:

$$\Gamma* = 3.8976 \times 10^{-9}\,\mathrm{mol\,cm^{-2}}.$$

Finally, the following formula can be used to calculate the electron transfer coefficient (α) of the reaction:

$$\mathrm{Ep} = \left(\frac{RT}{2\alpha f}\right)\ln v + constant$$

The amount of electron transfer amount for PSA electrooxidation obtained from the anode potential peak relationship in the scan logarithm of Figure S13C. α = 0.2284 from this value it can be concluded that the electrode diffusion process is irreversible in nature.

3.5 | Evaluation of selectivity

In order to validate the designed immuno-sensor, SWV, and DPV were recorded in the occurrence of various types of interferers such as HA, CEA, CA15-3, and SNCA mixed with PSA in equal proportions and PSA biomarker alone. When looking at Figure S14, it is clear that the electrochemical currents of the sensor-engineered immunoassay in the detection of PSA biomarkers are compared with the currents obtained from different types of interferers mixed with PSA. As shown in Figure S14, there are slight variations in the electrochemical signals which confirm that the interference of these species is insignificant. Therefore, the PSA target alone had the highest peak current, which was in DPV (2.21 μA) and SWV (5.17 μA). This acceptable

selectivity enhances our immunosensor designed to target PSA in real samples.

3.6 | Repeatability, Reproducibility and long-term stability of fabricated immunosensor

Stability and reproducibility have a significant role in analyzing the action of a sensor. It is important that an immunosensor be reusable in feasible usage such as instant clinical analysis and biological detection, which depends on the reproducibility and stability power of a biosensor. To study the efficiency of the prepared immuno-platform reproducibility, inter-day stability and cyclic stability with CV technique and intra-day stability with DPV and SWV techniques were examined. Reproducibility was checked out by employing 3 electrodes (Ab1-KCC-1-NH_2-DPA/AgNPs/P(CS)/GCE electrode) in the presence of supporting electrolyte 0.01 M $[Fe(CN)_6]^{3-/4-}$/KCl. The results showed that the prepared immunosensor has satisfactory reproducibility (Figure S15A,B (see supporting information)). To show the cyclic stability of the electrode substrate, a CV technique with the number of cycles (1, 5, 10, 50, 100) was used. Looking at the results, it turned out that our sandwich-type immunosensor showed up to 5 cycles of stability (Figure S16). Also, after storing the electrodes at 4°C for 3 days, the intermediate stability of the designed immunosensor was evaluated by measuring the peak current. Although after 48 hours the peak current of immunosensor has decreased, the engineered immunosensor showed great stability in 2 days (75%) (Figure S17). Figure S18 (see supporting information) also shows the inter-day stability of the immunosensor. Examination of the results shows that the developed immunosensor has maintained its stability for up to 80 minutes. But after 80 minutes, the stability of inter-day has decreased sharply and has almost lost its stability.

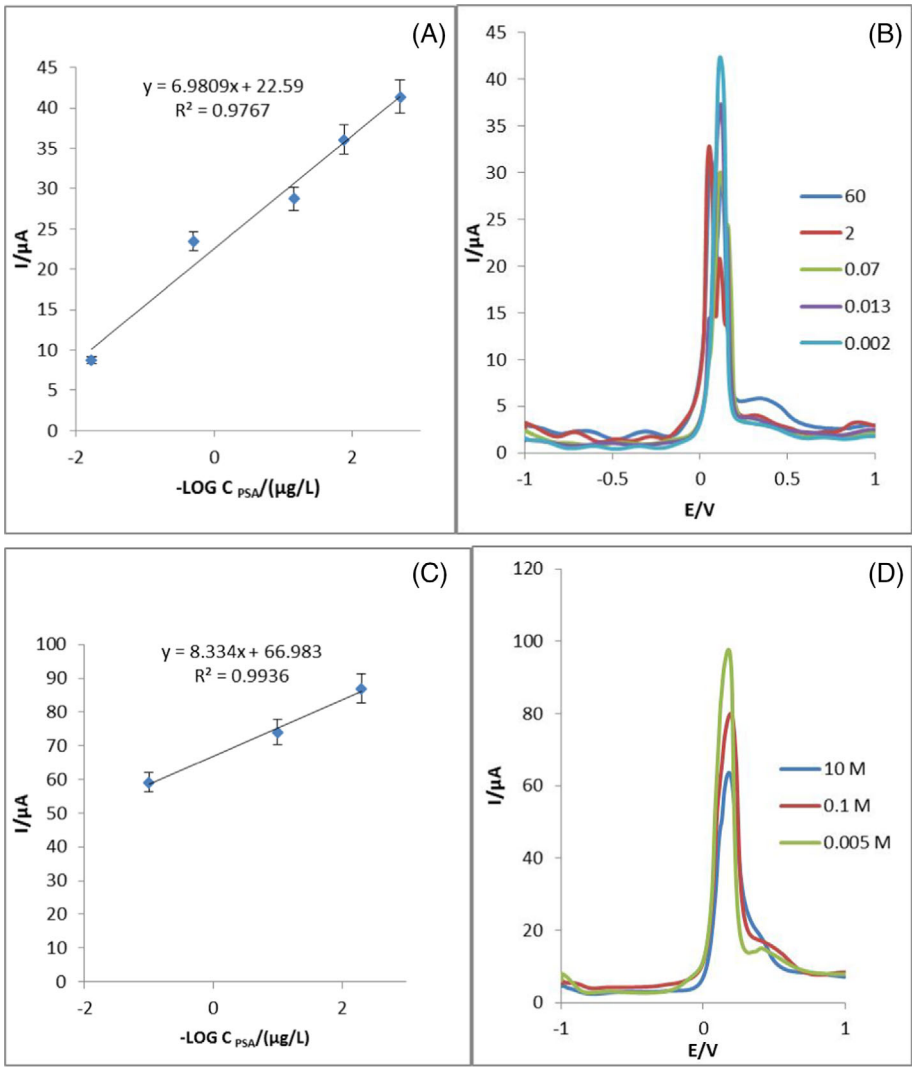

FIGURE 5 (A-C) DPVs and SWVs of different concentrations of biomarker (PSA) (0.002 µg L^{-1} – 0.005 µg L^{-1} – 0.008 µg L^{-1} – 0.013 µg L^{-1} – 0.03 µg L^{-1} – 0.07 µg L^{-1} – 0.1 µg L^{-1} – 2 µg L^{-1} – 10 µg L^{-1} – 30 µg L^{-1} – 60 µg L^{-1}) with human plasma samples in the presence of supporting electrolyte 0.01 M $[Fe(CN)_6]^{3-/4-}$/KCl, potential range −1 to 1 V and the scan rate of 100 mV/s. (B-D) related histograms

Another advantage of the proposed immunosensor was that the resulting modified electrode showed good long-term stability. Stability of the proposed electrode was tested by measuring the decrease in voltammetric current during repetitive DPV measurements of PSA with engineered immunosensor stored in −4°C. Obtained results show that this electrode has remarkable stability without significant change in the voltammetric currents. When the electrode was stored in the −4°C, the current response remained almost unchanged for about 8 days. RSD of repeated peak currents was (4.88%). The high stability of the immune-platform could be related to the strong affinity of P (CS) for AgNPs and the low solubility of the Ab1 encapsulated on KCC-1-NH-DPA in biological matrices. To check the inter-electrode reproducibility of the modified electrode, four modified electrodes were tested simultaneously by recording SWVs in the presence of supporting electrolyte, containing 10 PSA. The relative SD was 4.77%. Therefore, developed immunosensor imparts a suitable stability onto measurements of PSA by SWV and DPV techniques.

3.7 | Real sample analysis

To evaluate the possibility of application and measure the accuracy of the prepared immunosensor for clinical diagnosis, different concentrations of PSA (0.002, 0.005, 0.008, 0.013, 0.03, 0.07, 0.1, 2, 10, 30, 60 μg L^{-1}) was mixed to 5 μL of human plasma samples. DPVs and SWVs were recorded in the presence of supporting electrolyte 0.01 M $[Fe(CN)_6]^{3-/4-}$/KCl to continue. According to the results, the linear concentration range was between 0.002 to 60 μg L^{-1} and the result is 0.002 μg L^{-1} of LLOQ (Figure 5). Obtained results show the great linear relationship between the logarithm of PSA indicator concentration and peak current so that with decreasing concentration the peak current increases.

The linear regression equation achieved with each technique is as follows:

$$I_p\,(\mu A) = 6.9809 \log C_{(PSA)} + 22.59, R^2 = 0.9767\,(DPV)$$

$$I_p\,(\mu A) = 8.334 \log C_{(PSA)} + 66.983, R^2 = 0.9936\,(SWV)$$

4 | CONCLUSION

In summary, a sensitive sandwich-type immunosensor successfully developed to direct detection of PSA biomarkers in human plasma samples. Poly (chitosan) has been used as a substrate due to high adsorption power and excellent surface area and amine factionalized groups. AgNPs were deposited on the surface of biopolymer (P(CS)) as amplifiers of electron transfer current. Also, KCC-1-NH_2-DPA was employed as a great substrate for the encapsulation of biotinylated Ab1 of PSA with excellent properties. Finally, nanocomposite Cys A-AuNPs/TB/GLU/HRP-Ab2 has been employed as a current-enhancing probe for secondary antibody incubation. Under the optimal conditions, the obtained linear range was from 0.002 to 60 μg L^{-1} and the LLOQ was 0.002 μg L^{-1}. Due to the stated features of the immune-platform, the developed immunosensor is suggested to use in the clinical studies of prostate cancer detection.

ACKNOWLEDGEMENTS

The authors thank the financial support provided by the Tabriz University of Medical Sciences, Tabriz, Iran. Also, the authors thank Pharmaceutical Analysis Research Center, Tabriz University of Medical Sciences, as site of experimental research work.

CONFLICT OF INTERESTS

The authors declare no conflict of interests.

DATA AVAILABILITY STATEMENT

The data that support the findings of this study are available on request from the corresponding author. The data are not publicly available due to privacy or ethical restrictions.

REFERENCES

1. Siegel RL, Miller KD, Jemal A. Cancer statistics, 2016. *CA Cancer J Clin*. 2016;66:7-30.
2. Feng J, Li Y, Li M, et al. A novel sandwich-type electrochemical immunosensor for PSA detection based on PtCu bimetallic hybrid (2D/2D) rGO/g-C3N4. *Biosens Bioelectron*. 2017;91:441-448.
3. Pei H, Zhu S, Yang M, Kong R, Zheng Y, Qu F. Graphene oxide quantum dots@silver core–shell nanocrystals as turn-on fluorescent nanoprobe for ultrasensitive detection of prostate specific antigen. *Biosens Bioelectron*. 2015;74:909-914.
4. Zhou X, Yang L, Tan X, Zhao G, Xie X, Du G. A robust electrochemical immunosensor based on hydroxyl pillar[5]arene@AuNPs@g-C3N4 hybrid nanomaterial for ultrasensitive detection of prostate specific antigen. *Biosens Bioelectron*. 2018;112:31-39.
5. Çevik E, Bahar Ö, Şenel M, Abasıyanık MF. Construction of novel electrochemical immunosensor for detection of prostate specific antigen using ferrocene-PAMAM dendrimers. *Biosens Bioelectron*. 2016;86:1074-1079.
6. Liu Y. Electrochemical detection of prostate-specific antigen based on gold colloids/alumina derived sol-gel film. *Thin Solid Films*. 2008;516:1803-1808.
7. Yang Y, Yan Q, Liu Q, et al. An ultrasensitive sandwich-type electrochemical immunosensor based on the signal amplification strategy of echinoidea-shaped au@ag-Cu2O nanoparticles for prostate specific antigen detection. *Biosens Bioelectron*. 2018;99:450-457.
8. Morgan R, Boxall A, Bhatt A, et al. Engrailed-2 (EN2): a tumor specific urinary biomarker for the early diagnosis of prostate cancer. *Clin Cancer Res*. 2011;17:1090-1098.
9. Hu J, Wang S, Wang L, et al. Advances in paper-based point-of-care diagnostics. *Biosens Bioelectron*. 2014;54:585-597.
10. Chen Y, Yuan P-X, Wang A-J, et al. A novel electrochemical immunosensor for highly sensitive detection of prostate-specific antigen using 3D open-structured PtCu nanoframes for signal amplification. *Biosens Bioelectron*. 2019;126:187-192.
11. Pinwattana K, Wang J, Lin C-T, et al. CdSe/ZnS quantum dots based electrochemical immunoassay for the detection of phosphorylated bovine serum albumin. *Biosens Bioelectron*. 2010;26:1109-1113.
12. Wang R, Feng J-J, Liu W-D, Jiang L-Y, Wang A-J. A novel label-free electrochemical immunosensor based on the enhanced catalytic currents of oxygen reduction by AuAg hollow nanocrystals for detecting carbohydrate antigen 199. *Biosens Bioelectron*. 2017;96:152-158.

13. Shaban M, Hasanzadeh M. Biomedical applications of dendritic fibrous nanosilica (DFNS): recent progress and challenges. *RSC Adv*. 2020;10(61):37116-37133.
14. Behyar MB, Shadjou N. D-Penicillamine functionalized dendritic fibrous nanosilica (DFNS-DPA): synthesise and its application as an innovative advanced nanomaterial towards sensitive quantification of ractopamine. *RSC Adv*. 2021;11:30206-30214.
15. Polshettiwar V, Cha D, Zhang X, Basset JM. High-surface-area silica Nanospheres (KCC-1) with a fibrous morphology. *Angew Chem Int Ed*. 2010;49:9652-9656.
16. Polshettiwar V, Basset JM. High surface area fibrous silica nanoparticles. *USPATET*, US20110253643, 2010.
17. Hassanpour S, Saadati A, Hasanzadeh M. Sensitive monitoring of riboflavin in commercial multivitamins using poly (chitosan)-based nanocomposite. *J Mol. Recog*. 2020;33(2):e2817.
18. Haase A, Mantion A, Graf P, et al. A novel type of silver nanoparticles and their advantages in toxicity testing in cell culture systems. *Arch Toxicol*. 2012;86:1089-1098.
19. Li Z, Yin J, Gao C, Qiu G, Meng A, Li Q. The construction of electrochemical aptasensor based on coral-like poly-aniline and au nanoparticles for the sensitive detection of prostate specific antigen. *Sens Actuators B*. 2019;295:93-100.
20. He Y, Xie S, Yang X, Yuan R, Chai Y. Electrochemical peptide biosensor based on in situ silver deposition for detection of prostate specific antigen. *ACS Appl Mater Interfaces*. 2015;7:13360-13366.
21. Farshchi F, Hasanzadeh M, Mokhtarzadeh A. A novel electroconductive interface based on Fe3O4 magnetic nanoparticle and cysteamine functionalized AuNPs: Preparation and application as signal amplification element to minoring of antigen-antibody immunocomplex and biosensing of prostate cancer. *J Mol Recognit*. 2020;33(4):e2825.
22. Reddy YVM, Sravani B, Łuczak T, Mallikarjuna K, Madhavi G. An ultrasensitive rifampicin electrochemical sensor based on titanium nanoparticles (TiO2) anchored reduced graphene oxide modified glassy carbon electrode. *Colloids Surf A Physicochem Eng Asp*. 2021;608:125533.
23. Farschi F, Saadati A, Hasanzadeh M. A novel immunosensor for the monitoring of PSA using binding of biotinylated antibody to the prostate specific antigen based on nano-ink modified flexible paper substrate: efficient method for diagnosis of cancer using biosensing technology. *Heliyon*. 2020;6:e04327.
24. Farshchi F, Saadati A, Hasanzadeh M. An innovative Immunoanalysis strategy towards sensitive recognition of PSA biomarker in human plasma samples using flexible and portable paper based biosensor: a new platform towards POC detection of cancer biomarkers using integration of pen-on paper technology with immunoassays methods. *ImmunoAnalysis*. 2021;1:6.
25. Farshchi F, Hasanzadeh M, Solhi E. Immunosensing of prostate cancer in human plasma samples using immobilization of antibody on the surface of mesoporous silica-modified silver nanoparticles and its immunocomplex with prostate-specific antigen. *Anal Methods*. 2019;11:6159-6167.

SUPPORTING INFORMATION

Additional supporting information may be found in the online version of the article at the publisher's website.

How to cite this article: Behyar MB, Farshchi F, Hasanzadeh M. Sensitive recognition of prostate-specific antigen using biotinylated antibody encapsulated on *D*-penicillamine decorated wrinkled silicate nanoparticles (WSN): An innovative sandwich-type biosensor toward diagnosis of prostate cancer. *J Mol Recognit*. 2022;35(8):e2960. doi:10.1002/jmr.2960